

# Manufacturing of an absorbing filter controlled by a broadband optical monitoring

Bruno Badoil, Fabien Lemarchand\*, Michel Cathelinaud and Michel Lequime

*Laboratoire Institut Fresnel, Université Paul Cézanne, 13388 Marseille cedex 20 (France)*

\* Corresponding author: [fabien.lemarchand@fresnel.fr](mailto:fabien.lemarchand@fresnel.fr)

**Abstract:** This paper deals with a broadband optical monitoring set up useful for the manufacturing of absorbing coatings. The monitoring strategy consists in simultaneous measurements of transmittance and reflectance over a large spectral range. The resulting analysis allows then to determine the real time deposited thickness. A stage of design correction is possible after the deposition and analysis of each layer. This method has potential for thin metallic layers coatings. We then describe layer after layer the strategy for the control and manufacturing of a filter with given colorimetric properties.

© 2008 Optical Society of America

**OCIS codes:** 310.1620: Coatings, 310.3915: Metallic, opaque, and absorbing coatings, 310.1860: Thin films: Deposition and fabrication

---

## References and links

1. B. T. Sullivan and J. A. Dobrowolski, "Deposition error compensation for optical multilayer coatings. II. Experimental results - sputtering system," *Appl. Opt.* **32**, 2351-2360 (1993).
2. A. V. Tikhonravov, M. K. Trubetskov, and T. V. Amotchkina, "Investigation of the effect of accumulation of thickness errors in optical coating production by broadband optical monitoring," *Appl. Opt.* **45**, 7026-7034 (2006).
3. L. Li and Y. Yen, "Wideband monitoring and measuring system for optical coatings," *Appl. Opt.* **28**, 2890-2894 (1989).
4. A. V. Tikhonravov and M. K. Trubetskov, "On-line characterization and reoptimization of optical coatings," *Proc. SPIE* **5250**, 406-413 (2004).
5. D. Ristau, T. Gross, and M. Lappschies, "Optical broadband monitoring of conventional and ion process", in *Digest of Optical Interference Coatings on CD-ROM (Optical Society of America)*, paper TuE1 (2004).
6. M. Lappschies, B. Goertz, and D. Ristau, "Application of optical broadband monitoring to quasi rugate filter by ion beam sputtering", in *Digest of Optical Interference Coatings (Optical Society of America)*, paper TuE4 (2004).
7. S. Wilbrandt, R. leitel, D. Gabler, O. Stenzel, and N. Kaiser, "In situ broadband monitoring and characterization of optical coatings", in *Digest of Optical Interference Coatings on CD-ROM (Optical Society of America)*, paper TuE6 (2004).
8. B. T. Sullivan and K. L. Byrt, "Metal/dielectric transmission interference filters with low reflectance. 2. Experimental results," *Appl. Opt.* **34**, 5684-5694 (1995).
9. B. Badoil, F. Lemarchand, M. Cathelinaud and M. Lequime, "Interest of broadband optical monitoring for thin film filters manufacturing," *Appl. Opt.* **46**, 4294-4303 (2007).
10. S.D. Browning, J.A. Dobrowolski, "2007 OSA Topical meeting on Optical Interference Coatings manufacturing problem," paper MB1 (2007).
11. J. A. Dobrowolski, S. Browning, M. Jacobson, and M. Nadal, "2007 Topical Meeting on Optical Interference Coatings: Manufacturing Problem," *Appl. Opt.* **47**, 231-245 (2008).
12. O. Y. Borkovskaya, N. L. Dmitruk, and O. V. Fursenko, "Characterization of thin metal films with overlayers by transparency and multiangle including surface plasmon excitation reflectance ellipsometry method," *Proc. SPIE* **3094**, 250-254 (1997).
13. A. V. Tikhonravov, M. K. Trubetskov, O. F. Prosovskiy, and M. A. Kokarev, "Optical characterization of thin metal films," in *Digest of Optical Interference Coatings on CD-ROM (Optical Society of America)*, paper WDPDP2 (2007).
14. T. Csendes, B. Daroczy, and Z. Hantos, "Nonlinear parameter estimation by global optimization: comparison of local search methods in respiratory system modelling, *System Modelling and Optimization*," (Springer-Verlag, Berlin 1986) 188-192.

## 1. Introduction

The development and improvements of array detectors in the last twenty years have opened up new horizons for optical monitoring. The precise control of deposited thickness of thin film stacks is now possible using a real time analysis of the transmitted flux over an extended spectral range for dielectric [1-7] and metal/dielectric filters [8].

Typically, an in situ set up with at least a white light source and a Charged Coupled Device (CCD) or Photo Diode Array (PDA) detector enables acquisitions of the light passing through the coated substrate. Several techniques enable an efficient monitoring of the coated thickness. One example consists in finding the real time thickness by comparing the measured transmittance and the calculated spectral response as a function of layer thickness. This procedure can be repeated layer after layer. One main advantage of Broadband Optical Monitoring (BOM) is to be adapted to a large variety of designs, and specifically to non quarter wavelengths. The aim of this article is to demonstrate the efficiency of such a monitoring system on stacks including both metallic and dielectric materials. A simultaneous measurement of both transmittance and reflectance is very useful for monitoring such coating. To illustrate, we present the manufacturing of a filter with given color properties on both sides of the substrate.

## 2. Experimental set up

The dedicated vacuum coater uses the Reactive Low Voltage Ion Plating technology. This e-beam deposition process is assisted with Ar ions plasma. The following describes the start of the deposition of a layer: The first stage includes a pre-heating of the crucible with an electron gun for about 2 to 4 minutes under closed shutter. Last minute O<sub>2</sub> flow is on in the case of an oxide material. Then the Ar plasma is started, immediately followed by the opening of the crucible shutter. And finally, deposition starts.

The monitoring of thin metallic layers presents difficulties, especially if a dielectric oxide layer follows. Indeed, oxide layers require oxygen inside the chamber, and a partial oxidisation of the metal is possible. We will see in section 4 the corresponding modifications on the spectral response. An in situ BOM system measuring both transmittance and reflectance is an excellent tool to observe in situ the modifications of the optical properties of a thin metallic layer. In our monitoring set up described in Fig. 1, we use a tungsten halogen source ended by a 200  $\mu\text{m}$  diameter fibre. The source is imaged on the substrate with a spot diameter about 8mm and a negligible divergence. The substrate is then imaged on two fibres of 500  $\mu\text{m}$  diameter, corresponding to the transmittance and reflectance channels.

The two PDA detectors enable the recording of the spectra from 400 to 1000 nm with a signal to noise ratio of 3000 (respectively 1000) in transmittance (reflectance). A precise description of the set up performances is given in [9]. Note that the substrate, located at the periphery of the substrate holder, is at about 6 cm away from the center of the single rotary drive system. As a consequence, all the signal acquisitions need to be sequential, with an integration time of about 40 ms (signal time window) and a periodicity of 1.8s (rotary drive speed). By comparing measured and calculated spectra, the deposited thickness is sequentially evaluated. When the thickness estimation matches the theoretical design, the coating is stopped. At the end of the deposition of a layer, if the deposited thickness is not exactly the one expected, a procedure consisting in correcting the design of following layers can be applied.

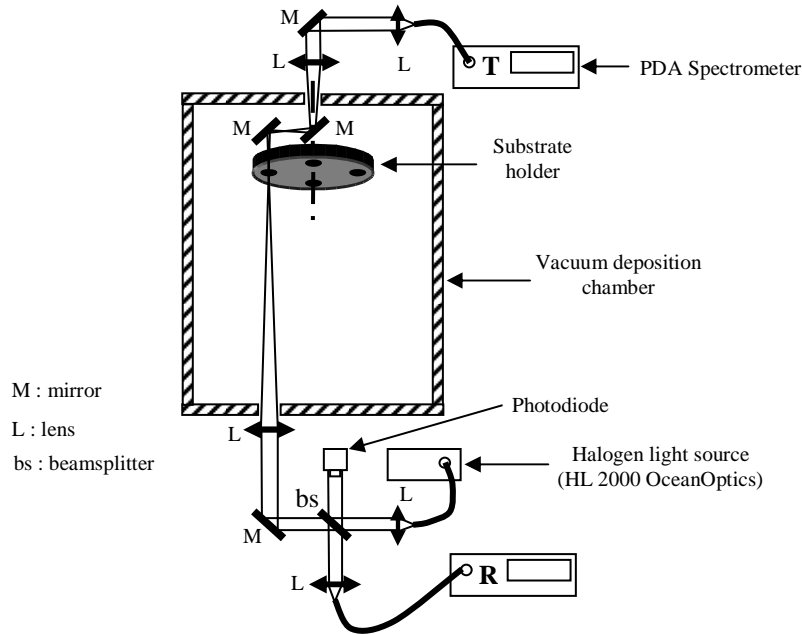


Fig. 1. BOM set up implanted on a Balzers Ion Plating deposition machine

### 3. Design of an absorbing filter with given properties

In order to illustrate the potentialities of our monitoring system, we decided to design and manufacture a filter with given colorimetric properties, following the manufacturing problem of OIC 2007 conference [10-11]. The precise characteristics (intensity and colorimetry) are given in table 1.

Table 1. characteristics of a colorimetric filter – from [9]

CIE standard observer color coordinate targets	$x_m^T$	$y_m^T$	$Y_m^T$	<b>m</b>
Unpolarized light reflected from side 1 (backside)	0.16	0.25	0.3	1
Unpolarized light reflected from side 2 (filter side)	0.5	0.45	0.3	2
Unpolarized light transmitted	0.31	0.31	0.3	3

The merit function for the manufacturing contest was given by (1).

$$MF = \left\{ \frac{1}{9} \left[ \sum_{m=1}^3 \left( \frac{x_m^T - x_m}{0.01x_m^T} \right)^2 + \sum_{m=1}^3 \left( \frac{y_m^T - y_m}{0.01y_m^T} \right)^2 + \sum_{m=1}^3 \left( \frac{Y_m^T - Y_m}{0.01Y_m^T} \right)^2 \right] \right\}^{1/2} \quad (1)$$

We chose to look at a single side coated design, named filter side. The residual absorption of 40% and the difference of color between the two reflected sides impose to look for designs including at least one absorbing layer. We selected hafnium oxide (HfO<sub>2</sub>, named H material) and silica oxide (SiO<sub>2</sub>, named L material) as dielectric materials and hafnium (Hf, M material) as absorbing material. The accuracy of the estimated refractive index of oxide dielectric materials is better than for metallic materials. A mere Cauchy law (2) describes the estimation of oxide indices on the visible range fairly well.

$$n(\lambda) = a_0 + \frac{a_1}{\lambda^2} + \frac{a_2}{\lambda^4} \quad (2)$$

With  $a_0 = 2.0739$ ,  $a_1 = 1.8054 \cdot 10^4 \text{ nm}^2$ ,  $a_2 = -3.4792 \cdot 10^8 \text{ nm}^4$  for HfO<sub>2</sub>  
and  $a_0 = 1.4686$ ,  $a_1 = 5.3790 \cdot 10^3 \text{ nm}^2$ ,  $a_2 = -2.3097 \cdot 10^8 \text{ nm}^4$  for SiO<sub>2</sub>

For these materials,  $k(\lambda)$  is very close to 0 ( $k < 10^{-4}$  in the visible range) and is therefore taken to be null.

The index of a semi transparent metallic film is estimated either on ellipsometric methods [12], or spectro-photometry [13]. The latter consists in fitting a theoretical model on reflectance and transmittance curves of a bi-layer (Hf - HfO<sub>2</sub>). As the refractive index of HfO<sub>2</sub> is supposed to be known, one has to look for thicknesses of the two layers and optical constant of Hf using the spectral curves. Following this approach, we have decided to use a Cauchy model for  $n$  and for  $k$ . A reverse engineering procedure gives the following values for Hf:

$a_0 = 3.709$ ,  $a_1 = -2.670 \cdot 10^5 \text{ nm}^2$ ,  $a_2 = -1.231 \cdot 10^9 \text{ nm}^4$  for  $n$ , real part of Hf index  
 $a_0 = 3.346$ ,  $a_1 = -5.322 \cdot 10^5 \text{ nm}^2$ ,  $a_2 = 6.045 \cdot 10^{10} \text{ nm}^4$  for  $k$ , imaginary part of Hf index

This characterization does not take into account possible inhomogeneities of the metallic layer. The optical constants are supposed to be homogenous for both metallic and dielectric layer. Consequently, if the metallic layer is partially oxidised, the contribution of the refractive index gradient is included into the homogeneous model.

One possible issue, considering thin metallic layers, is that the optical constants  $n$  and  $k$  are dependant on the deposited thickness. Our experimental knowledge on thin Hf layers is related to the deposition of light absorbers for spatial applications. In this case, we have considered thickness varying from 7 to 20 nm. The determination of refractive indices in this range of thicknesses does not lead to significant changes. However, the difference with an opaque (thickness more than 100nm) layer is significant, where for an opaque Hf layer  $n$  and  $k$  are noticeably higher.

Under these indices conditions, we sought a design including H,M,L layers and corresponding to the lowest MF. We used a global optimization algorithm derived from [14]. Briefly, it is a clustering method that evaluates random initial designs, and then seeks several local minima with a Quasi Newton algorithm. The best result is called global minimum. For the initial design, the requirement is to provide the number of layers and the appropriate chain of materials. We choose a sequence of 8 layers substrate-H-L-H-L-H-L-M-H-air. For the following, this design presents two advantages: a single metallic layer and a positioning of this layer near the air. As the accuracy of refractive index determination is better for dielectric materials, it is preferable to insert only one Hf layer. Note also that after a metallic layer, the monitoring of the following layers is rendered more difficult and less precise. With such a design, only a single layer will be coated after the metallic one. The optimization program finally provides the theoretical design given in table 2. The merit function is about 6.61, and the colorimetric coordinates are given in table 3.

Table 2. Colorimetric filter structure

	thicknesses (nm)	materials
layer 1	179.6	H
layer 2	259.6	L
layer 3	58.5	H
layer 4	253.6	L
layer 5	77.8	H
layer 6	19.9	L
layer 7	11.7	M
layer 8	145	H

Table 3. Colorimetric characteristics of filter defined on table 2

CIE standard observer color coordinate targets	$x_m^T$	$y_m^T$	$Y_m^T$	m
Unpolarized light reflected from side 1 (backside)	0.160	0.261	0.261	1
Unpolarized light reflected from side 2 (filter side)	0.449	0.444	0.300	2
Unpolarized light transmitted	0.341	0.315	0.303	3

On the Fig. 2, one can observe the expected spectral responses in transmittance (red curve) and in reflectance (filter side – blue curve, backside – green curve).

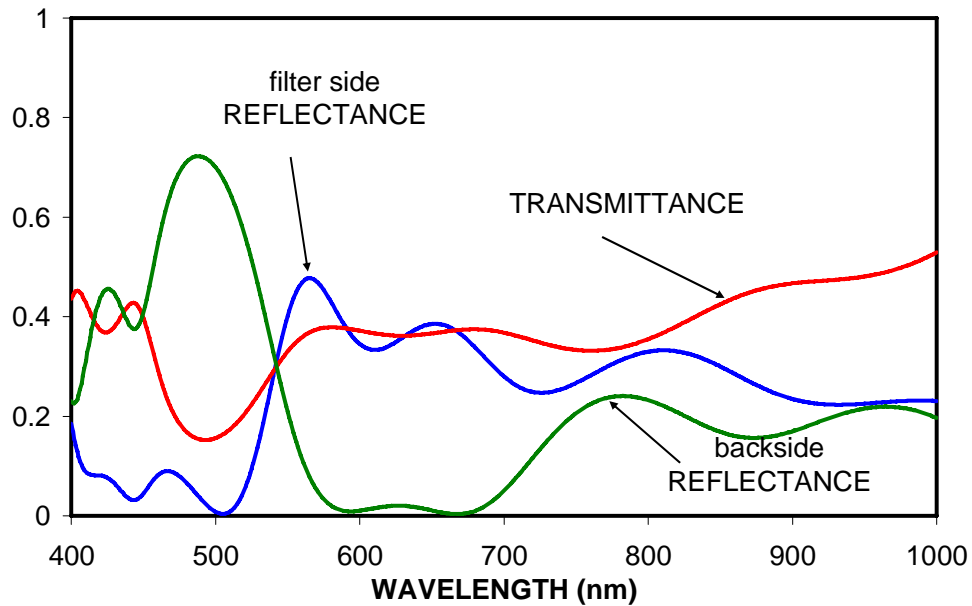


Fig. 2. Theoretical spectral responses of the colorimetric filter design described in Table 2.

#### 4. Manufacturing of the filter

Our monitoring strategy consists in evaluating the real time deposited thickness from reflectance and transmittance data. The simultaneous measurement of transmittance and reflectance is not mandatory as it is the case for optical characterization of metallic film, but it provides additional information on the absorption level of the filter, and facilitates the monitoring of the last layer.

The design can be corrected taking into account new values of thicknesses already deposited, allowing a compensation of thickness errors. The deposition of the 8-layers stack is performed as followed: for the first 6 dielectric layers, residual errors on thickness are negligible (below 0.5 nm in absolute value). Results for the first 6-layers are presented in Fig. 3. Note that we have represented transmittance and reflectance for a semi infinite substrate. The influence of backside is then subtracted.

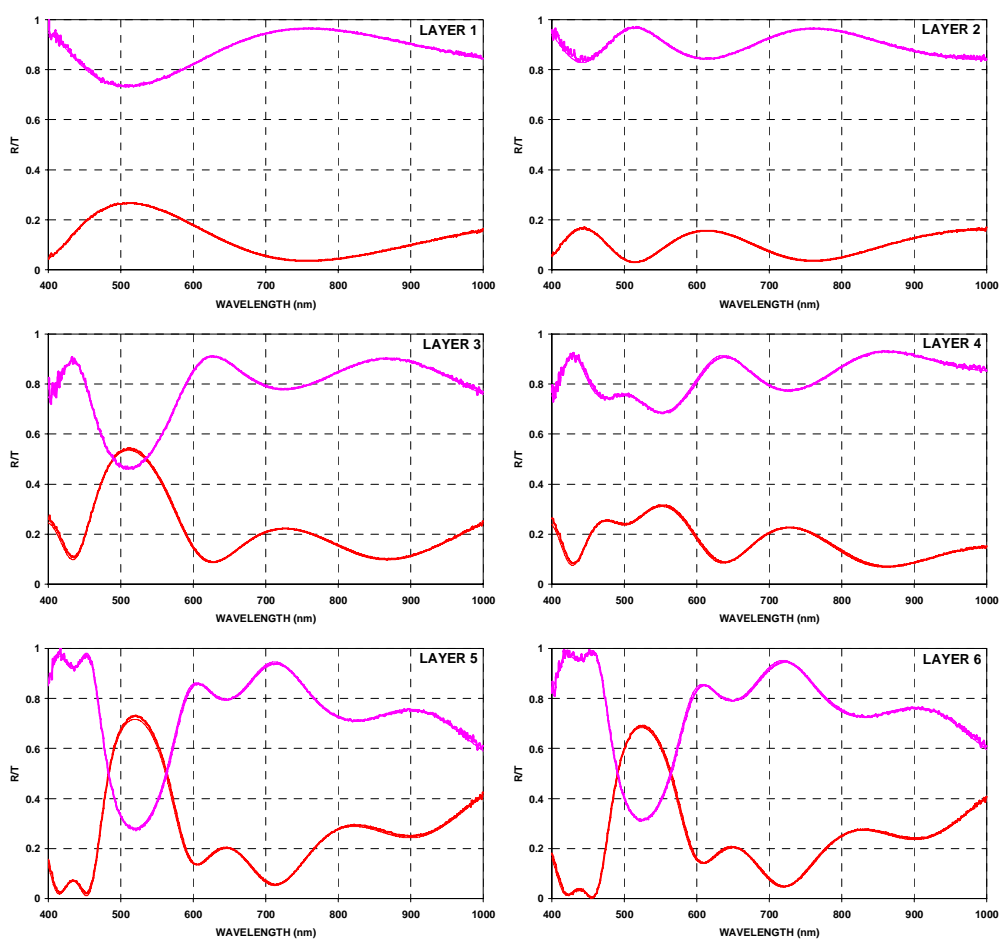


Fig. 3. Experimental reflectance and transmittance of the first 6 layers. Theoretical responses are in thin lines.

The monitoring of the 7<sup>th</sup> layer is the most problematic. First of all, the deposition is very fast (about 30 seconds), and second of all, the metallic layer is altered by 2 factors: the

introduction of oxygen inside the vacuum chamber before the deposition of layer 8 and the triggering of the Ar plasma as soon as the deposition of layer 8 begins.

Our strategy consists in performing the evaluation thickness of layer 7 once the layer 8 deposition starts. We thus take into account the two factors cited above and influencing drastically the metal thickness evaluation. Figure 4 shows the spectral responses at the end of the deposition of layer 7, after the introduction of oxygen, and at the triggering of the Ar plasma. One can also see the fit between theoretical and experimental spectra when a thickness of 11.3nm of a homogenous metallic layer is considered. 11.3nm is our thickness estimation and is not very different from the target thickness (11.7nm).

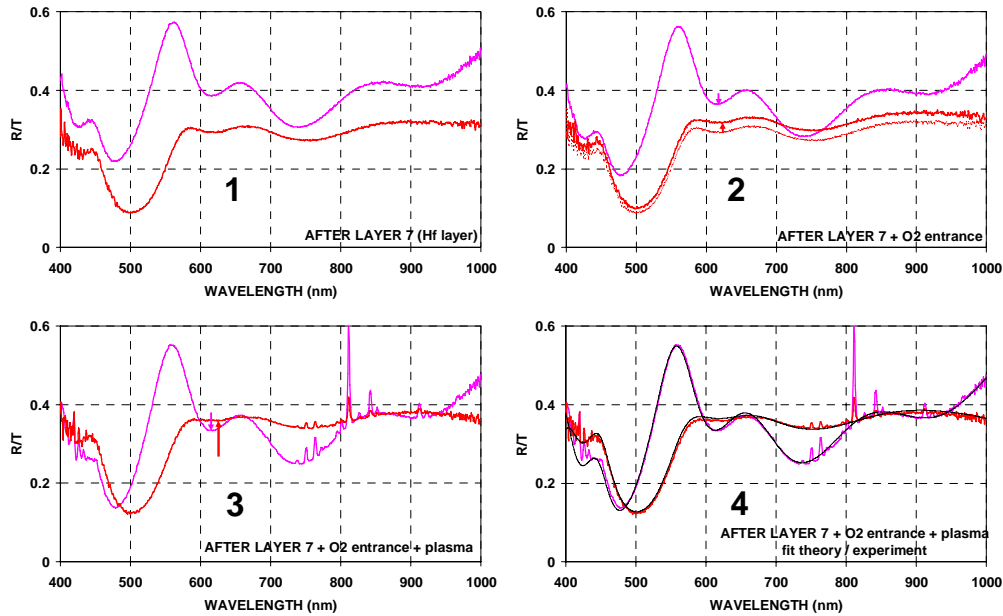


Fig. 4. Reflectance and Transmittance from the end of layer 7' deposition to the beginning of layer 8' deposition.

It is judicious to optimize the layer 8 by the merit function MF (Eq. (1)). As our set up measures the reflectance only on the filter side, we use a truncated merit function with the two measured spectra (see Eq. (3)).

$$TMF = \left\{ \frac{1}{6} \left[ \sum_{m=2}^3 \left( \frac{x_m^T - x_m}{0.01x_m^T} \right)^2 + \sum_{m=2}^3 \left( \frac{y_m^T - y_m}{0.01y_m^T} \right)^2 + \sum_{m=2}^3 \left( \frac{Y_m^T - Y_m}{0.01Y_m^T} \right)^2 \right] \right\}^{1/2} \quad (3)$$

The deposition process is stopped when the experimental TMF is at its minimum value. The final spectra are given in Fig. 5. The good agreement between theoretical and experimental curves indicates that the modelling of the metallic layer as an homogeneous layer is a good approximation for such filter. We evaluate the total merit function defined by (1), including backside reflectance to a value of MF = 7.03.

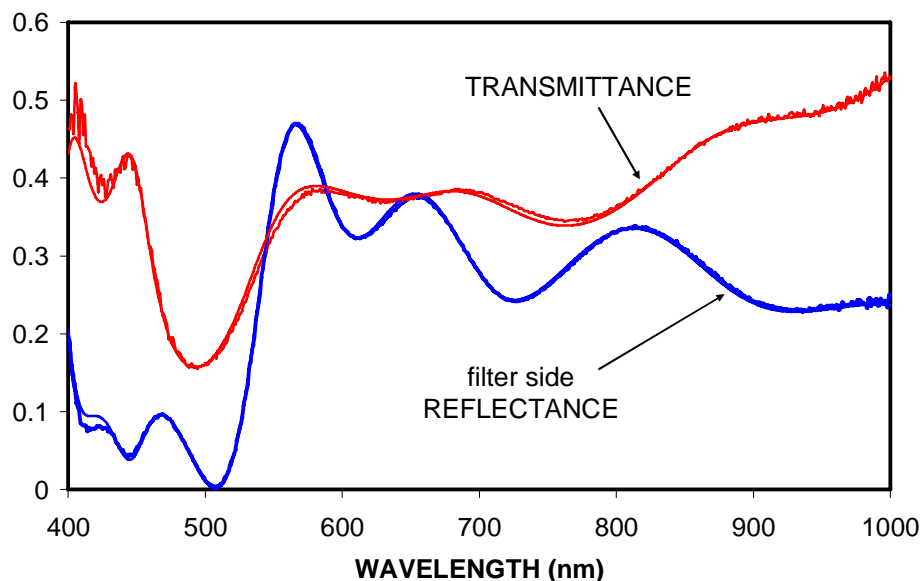


Fig. 5. Reflectance and transmittance of the 8-layer-filter. Experimental spectra are in bold lines, theoretical values are in thin lines.

Considering the good fit between theoretical and experimental curves, we now try to reduce the merit function by adding new layers. Our global optimization program gives us a solution with three additional layers given in table 4, where the new layers are in bold font. The new merit function would be  $MF = 5.36$ . Such a theoretical improvement permits to try the additional deposition. We use the same monitoring process as previously described. The last layer is monitored by the minimum of TMF (see Eq. (3)). The final experimental and theoretical spectral responses measured with a commercial spectrophotometer (Perkin Elmer Lambda 18) are shown in Fig. 6, the experimental merit function is  $MF = 5.7$ .

Table 4. Improved colorimetric filter design. Additional layers are in bold font

	<b>thicknesses (nm)</b>	<b>materials</b>
layer 1	179.8	H
layer 2	260	L
layer 3	58.4	H
layer 4	254.3	L
layer 5	77	H
layer 6	20.5	L
layer 7	11.3	M
layer 8	146.5	H
layer 9	<b>81.9</b>	L
layer 10	<b>74.6</b>	H
layer 11	<b>66.8</b>	L



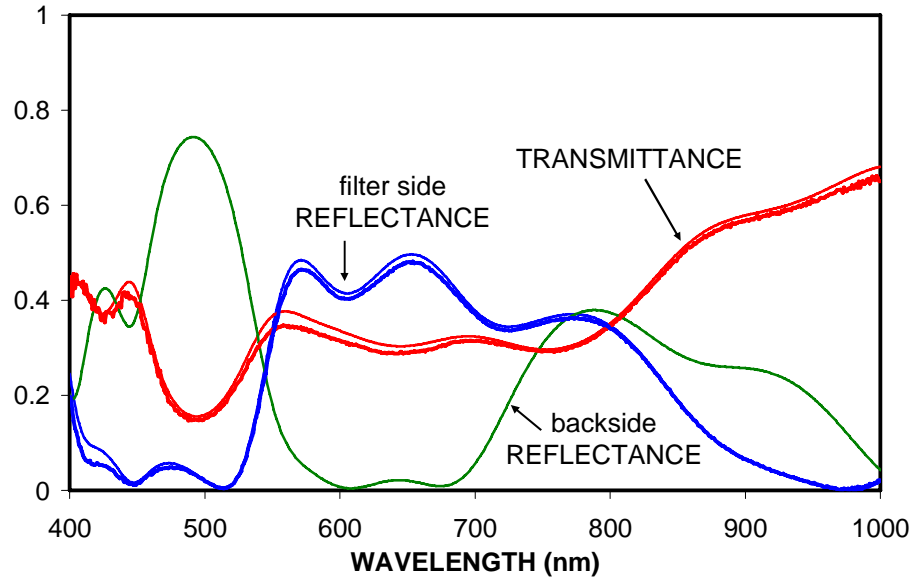


Fig. 6. Spectral responses of the colorimetric filter after the 3 additional layers: transmittance (red curve), reflectance (filter side-blue curve), backside reflectance (green curve). Experimental measurements are in bold lines, theoretical values are in thin lines.

From spectral measurements we deduce the colorimetric parameters given by table 5. Figure 7 is a picture of the final component illuminated by the sun.

Table 5. Colorimetric parameters

<b>m</b>	<b>CIE standard observer color coordinate targets</b>	$x_m^{th}$	$x_m^{mesure}$	$y_m^{th}$	$y_m^{mesure}$	$Y_m^{th}$	$Y_m^{mesure}$
1	Unpolarized light reflected from side 1 (backside)	0.160	0.159	0.250	0.262	0.300	0.256
2	Unpolarized light reflected from side 2 (filter side)	0.500	0.493	0.450	0.443	0.300	0.296
3	Unpolarized light transmitted	0.310	0.327	0.310	0.318	0.300	0.287

$x_m^{th}$ ,  $y_m^{th}$  et  $Y_m^{th}$  : theoretical colorimetric parameters,  $x_m^{mesure}$ ,  $y_m^{mesure}$  et  $Y_m^{mesure}$  : colorimetric parameters calculated from measurements

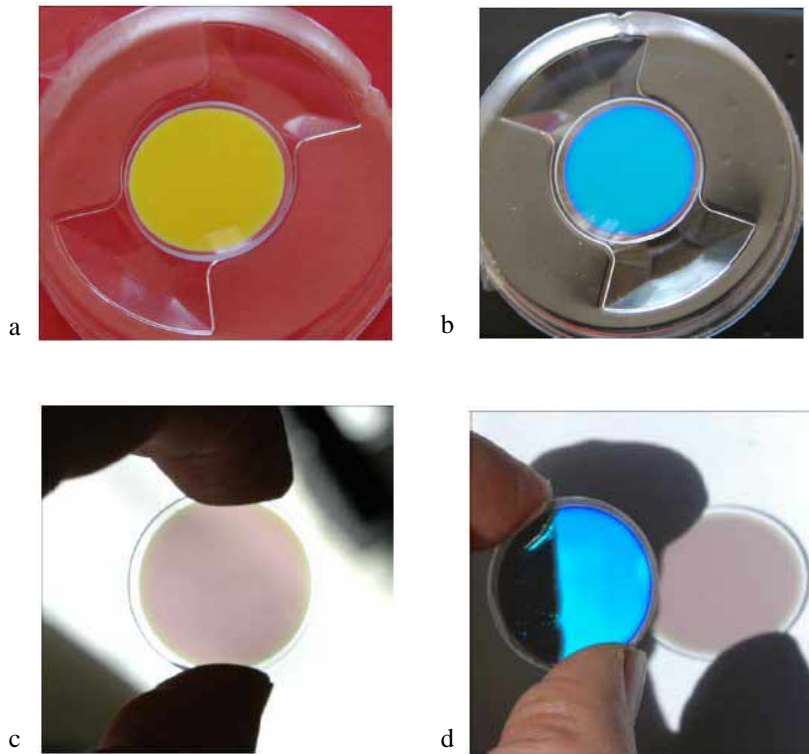


Fig. 7. Reflected colors on filter side (a) and backside (b et d), and transmitted color (c et d).

## 5. Conclusion

Thin film filters including thin metallic layers are extremely difficult to monitor. Complex phenomena occur probably due to a partial oxidation of the metal when an oxide is deposited after. The real metallic deposited thickness is then difficult to estimate. The simultaneous measurement of reflectance and transmittance over a large spectral range is an efficient tool to analyse the metal optical properties variations. Our approach consisted in modelling the metallic layer as an homogeneous layer of optical constants determined on a bi layer stack. Its thickness was then determined after the following layer deposition started.

By combining analysis and design, it is also possible to modify the thicknesses of next layers in order to improve the merit function. We have successfully applied this strategy for manufacturing a colorimetric filter with given properties.

In the future, we plan to improve our results by proceeding in a real time optimization of the optical constant (refractive index). The benefit should be substantial in the case of semi-transparent metallic layers whose oxidation phenomenon probably depends on several factors such as temperature and  $O_2$  pressure.